Electroweak Physics at CDF

The CDF Collaboration[1]

Presented by James R. Bensinger
Brandeis University

Abstract

The cross section for production and decay of the intermediate vector boson, $W \rightarrow e\nu$, has been measured in 1.8 TeV proton-antiproton collisions in the Collider Detector at Fermilab. An analysis of events with missing transverse energy greater than 25 GeV and with an electron with transverse energy greater than 15 GeV from a data sample of 25.3 nanobarns^{-1} yields $\sigma \cdot B = 2.6 \pm 0.6 \pm 0.5$ nanobarns.

1. Introduction

One of the clear goals for modern hadron colliders is a detailed and systematic study of the standard model. Such measurements will help pin down the as yet unknown parameters of the standard model and, with luck, point toward advancements beyond the standard model. As a first step in this effort we present the results on W production from the 1987 data run of the Collider Detector at Fermilab.

2. Detector Overview

The CDF detector has been well described elsewhere.[2] The parts of the detector that are particularly important for this analysis are the central tracking chamber (CTC) and the calorimeters, the electromagnetic (EM) and hadronic (HAD) calorimeters, and the beam-beam counters (BBC).

The CTC is an axial wire drift chamber (60 axial and 24 small angle stereo layers) in a 1.5 Tesla magnetic field. Both the CTC and magnetic field are aligned with the beam axis. The CTC is used to measure the charged particle momenta. Its measurement accuracy was approximately 200 microns, which gives a resolution of $\delta P_t/P_t^2 = 0.002\ (\mathrm{GeV}/c)^{-1}$.

Outside the CTC are the electromagnetic and hadronic calorimeters. These are arranged in a fine-grained projective geometry which extends to within 2 degrees of the beam pipe in either direction. The calorimetry is organized by region: The "central" and "endwall" region (pseudorapidity or $|\eta|<1.1$), the "plug" region ($1.1<|\eta|<2.4$) and the forward region

($2.4<|\eta|<4.2$). The central and endwall calorimeters EM (HAD) use a scintillator lead (iron) sandwich design with a tower granularity of $\delta\eta=0.1$ and $\delta\phi=15°$. The EM calorimeters in the central region have wire chambers with cathode strips (strip chambers) at shower maximum to provide an accurate measurement of the shower centroid. The plug and forward calorimeters have gas proportional tube lead (iron) sandwich construction with $\delta\eta=0.1$ and $\delta\phi=5°$. Electrons for this analysis were required to be in the central detector, while calorimetry with $|\eta|<3.6$ was used for the missing E_t calculation. Beyond $|\eta|=3.6$ CDF does not fully contain jets.

At each end of the detector there are scintillation counters which cover the region $3.2<|\eta|<5.9$, the BBC system. These counters are used for triggering and luminosity monitoring. The principal contribution to the systematic error in the cross section measurement will be the error in luminosity due to uncertainty in extrapolating cross sections from lower energies.

Events were triggered by requiring that there be at least one hit in the BBC's on each side of the detector and that there be an $E_t>15$ GeV of electromagnetic energy in a single central "trigger" tower of $\delta\eta\times\delta\phi=0.2\times15°$. In addition minimum bias data were taken simultaneously to monitor the detector and make small corrections to the data.

3. Data Analysis

The results presented here are based on 4×10^5 recorded events corresponding to a total luminosity of 25.3 nanobarns^{-1}. The analysis followed two complementary paths: (1) identification of the missing E_t and (2) identification of the electron. In each analysis tight cuts were used on the object of study and loose cuts on the other object. These two analysis paths ended up with the same set of events, but during the course of the analysis the backgrounds at any stage were quite different. This approach is important for understanding the performance of a new detector and providing a cross check on backgrounds and efficiencies.

The missing E_t is defined as

$$\not{E}_t \equiv \sum_{\text{Towers}} \vec{E}_t \text{ (EM+HAD)} \qquad |\eta| < 3.6$$

where the sum includes all towers above threshold[3] while the E_t is the scalar sum for $|\eta|<2.4$. The cuts for the missing Et analysis are shown in the table below.

Cuts for the $\not{E}_t$ Analysis	
Cut	Number of Events
$\not{E}_t \geq 25$ GeV	4178
1 Central Cluster $E_t(EM) \geq 15$ GeV	1604
$\frac{\not{E}_t}{\sqrt{E_t}} > 2.8$	115
Loose Electron Cut $\frac{E}{p} < 2;\ \frac{E_{EM}}{E_{EM}+E_{HAD}} > .85$	22

Cut 2 is based on a clustering algorithm[4] which merges a seed tower with $E_t > 1.0$ GeV to adjoining towers above a 0.1 GeV threshold. From the minimum bias studies the missing E_t resolution is $\sigma_{RMS} = 1.0*\sqrt{(Et)}$. One additional event failed the loose electron cut with an E/p>2. Radiative W decay calculations indicate that 3±1% of the electrons should radiate more than 50% of their energy.

For the electron analysis we define the isolation, I(R), of the electron to be the E_t outside the electron cluster but inside a ring in η-ϕ space of radius $R=\sqrt{\{(\eta-\eta_e)^2+(\phi-\phi_e)^2\}}$ about the electron cluster η_e and ϕ_e divided by the electron cluster E_t.

$$I(R) = \frac{\left[\sum_{\eta,\phi<R} E_t(\text{towers}) - E_t(e)\right]}{E_t(e)}$$

Tracking requirements included a good matching between that shower centroid in the strip chambers and the CTC track. A major background is QCD jet events where one jet mimics an electron. To reduce this background we eliminate events which have a cluster with $E_t > 5$ GeV back to back (180°±30° in ϕ) with the electron candidate, the di-jet cut. The cuts and numbers of surviving events for this analysis are listed in table below. In addition to the events listed here there are 6 additional events which have a second EM cluster with a large e-e mass. These events are Z° candidates.

The distribution of E/P is shown in figure 1 for the W candidates. Figure 2 plots the missing E_t verses E_t for events in the electron analysis path. This figure shows a clear separation of the W events.

Cuts for the Electron Analysis	
Cut	Number of Events
EM Cluster : $E_t > 15$ GeV ; $\frac{HAD}{EM} < .05$; I (R<.4) < .1	3753
Good Track : $\frac{E}{P} < 2$; $\delta\phi$ (| track - strip |) < 3.0 cm	137
Di-jet: No cluster $E_t > 5$ GeV Opposite $\pm 30°$ in ϕ.	61
$\not{E}_t > 25$ GeV	21

All of the events found in the electron analysis were also found in the missing E_t analysis. The one event found in the missing E_t analysis but not in the electron analysis failed on a track quality cut. We take all 22 events found in either analysis path as our final W sample.

4. Backgrounds and Efficiencies

The backgrounds studied fell into three broad categories: experimental effects, event related processes, and physics backgrounds. The first category includes the following: (1) Cosmic rays which were eliminated by a timing window of 20 nanoseconds on the hadron TDC's. (2) Particles from the Main Ring which enter the calorimeters while data is being taken. The Fermilab Main Ring goes over the detector along the top of the hall and runs continuously to produce antiprotons while the Tevatron is in operation. This background was also eliminated by the the timing cuts. (3) "Spikes" in the calorimeters including cable pickup, single phototube pulses, and discharges and knock-on protons in the gas calorimetry. These were eliminated with topological cuts that identified these signals as not consistent with real particle showers.

The second class of backgrounds is due to events where some combination of $\pi^{\pm} + n\gamma$ ($n \geq 0$) emulates the electron signal. These effects were studied by loosening cuts and understanding how the background grows. From these studies we estimate that this background in the electron analysis is 0.6±0.3 events and in the missing E_t analysis is < 0.2 events. In addition it is possible that the semileptonic decay of top quarks or the decay $W \rightarrow \tau\nu_\tau$ ($\tau \rightarrow e\nu\nu$) could look like direct W decay. These backgrounds were investigated using Monte Carlo techniques. For any top mass these studies found that the top background was < 0.2 events. The τ decay of the W contributes 0.6±0.2 events.

The losses due to the pseudorapidity cut, various thresholds, and the gaps between calorimeter modules were found from Monte Carlo studies. The error in the pseudorapidity

correction is primarily due to the uncertainty in the structure functions. A table of efficiencies is given below:

Selection Efficiencies		
	Missing E_t	Electron
Rapidity Cut	0.50 ± 0.05	
Edges of Calorimeter Modules	0.91±0.01	
Thresholds	0.84±0.02	
Di-jet Cut	0.92±0.02	
Radiative Corrections	0.97±0.01	
Spurious Clusters	0.985±0.01	
Trackings Cut		0.98±0.02
HAD/EM Calorimetry Cut		0.96±0.04
Isolation Cut		0.99±0.01
Timing Cut	0.99±0.01	
Total	0.33±0.04	0.31±0.04

5. Results

From a data sample with the integrated luminosity, backgrounds, and efficiencies indicated above, we obtain a measurement of the cross section times branching ratio for W production of

$$\sigma_W \cdot B(W \rightarrow e\nu) = 2.6 \pm 0.6 \pm 0.5 \text{ nanobarns.}$$

The first error is statistical and the second is systematic, primarily coming from the error in the extrapolating cross sections from lower energy measurements in the luminosity calculation. This result is shown in figure 3 along with lower energy measurements.[5] The data is in good agreement with theoretical predictions.[6] The transverse mass is defined by

$$M_T = \sqrt{2 \cdot E_T^e \cdot E_T^\nu \cdot [\, 1 - \cos(\delta\phi_{e\nu})\,]}$$

and the distribution in transverse mass is shown in figure 5. A fit to the transverse mass spectra predicted by Isajet[7] gives a W mass of

$$M_W = 80.0 \pm 3.3 \pm 2.4 \text{ GeV/c}^2$$

where the first error is statistical and the second is systematic. The principal contribution to the systematic error is is the uncertainty in the energy scale.

The P_t of the W is defined by

$$P_t(W) = |\vec{P}_t(e) + \vec{\not{E}}_t|$$

where the momentum of the electron is from the calorimeter measurement. The effect of the various (missing E_t) cuts, in particular the di-jet cut, has been studied by Monte Carlo simulation. The $P_t(W)$ dependence on the efficiency is not very strong, at least in the P_t range available with the present statistics. The results for the Pt(W) distribution are shown in figure 5. For comparison we also show the theoretical predictions[8] at y = 0.0 and $\sqrt{s}$ = 0.63 and 1.8 TeV. The theoretical curves include the effects of our detector resolution. Clearly a larger sample of events is needed before any conclusions can be drawn.

6. Summary

From the 1987 CDF run, which collected a data sample of 25.3 nanobarns^{-1}, we find that $\sigma \cdot B(W \rightarrow e\nu) = 2.6 \pm 0.6$ (statistical) $\pm$ 0.5 (systematic). This result is consistent with previous measurements and theoretical predictions. We also present the $P_t(W)$ distribution along with theoretical predictions.

This work would not have been possible without the skill and hard work of the accelerator division of Fermilab. We thank the staffs of our institutions for their many contributions to the construction of the detector. This work was supported by the U.S. Department of Energy, the National Science Foundation, Istituto Nazionale di Fisica Nucleare, The ministry of Science, Culture, and Education of Japan, and the A. P. Sloan Foundation.

Figure Captions

Figure 1 Distribution of calorimeter energy divided by track momentum for W candidates.

Figure 2 Distribution of missing E_t verses E_t for the events found in the electron path.

Figure 3 The cross section times branching ratio for $W \rightarrow e\nu$ versus center of momentum energy. The prediction is from reference 6 adjusted for a W mass of 80 GeV/c^2.

Figure 4 The distribution in transverse mass for the W candidate events. The curve is an ISAJET prediction for a W mass of 80 GeV/c^2.

Figure 5 Distribution of $P_t(W)$ corrected for efficiency. The curves shown are theoretical predictions from reference 8 convoluted with our experimental resolution.

---

[1] ANL-Brandeis-U of Chicago-Fermilab-INFN,Frascati-Harvard-U of Illinois-KEK-LBL-U of Pennsylvania-INFN,Pisa-Purdue-Rockefeller-Rutgers-Texas A&M-Tsukuba-U of Wisconsin.

[2] F. Abe et al., NIM A271, pg. 387 (1988) and references therein.

[3] The single tower thresholds are (in GeV): 0.1 for the Central EM; 0.2 for the Central HAD; 0.5 for the Plug EM, HAD, and Forward EM; and 0.8 for the Forward HAD.

[4] The clustering algorithm is described in a talk given by S. Kim, Proc. Physics in Collisions 7, Tsukuba (1987).

[5] C. Albarjar et al., Phys. Lett. 198B, 271 (1987); G. Arnison et al., Phys. Lett. 122B, 1-3 (1983); M. Banner et al., Phys. Lett. 122B, 476 (1983).

[6] G. Altarelli, K. Ellis, M. Greco, G. Martinelli, Nucl. Phys. B246, 12 (1984); G. Altarelli, K. Ellis, G. Martinelli, Z. Phys. C27, 617 (1985).

[7] F. Paige and S. D. Protopopescu, BNL 38034 (1986).

[8] Altarelli et al., Z. Phys. C27, 617 (1985).

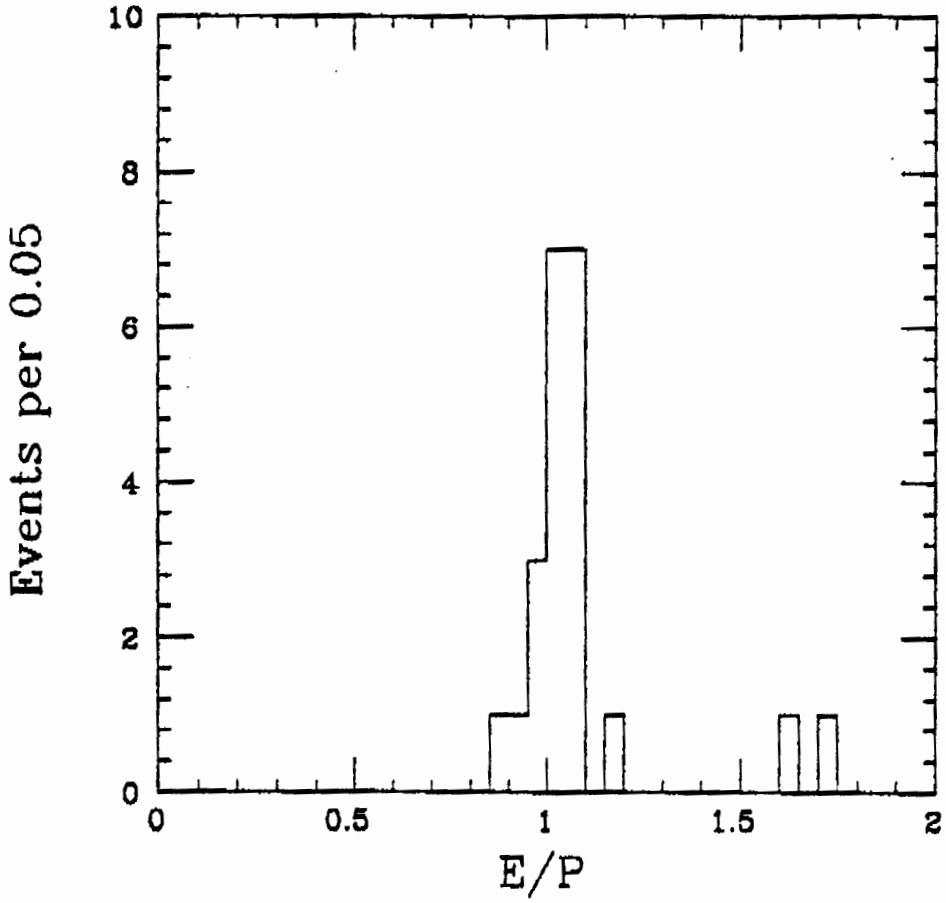

FIGURE 1

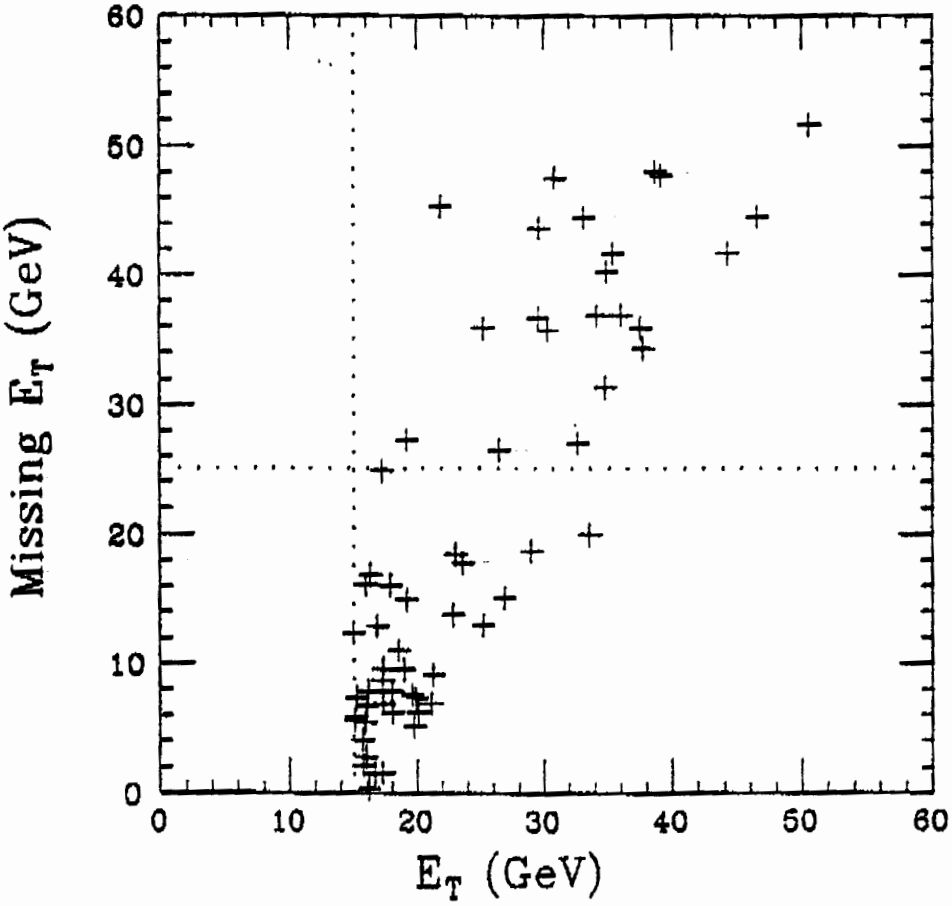

FIGURE 2

FIGURE 3

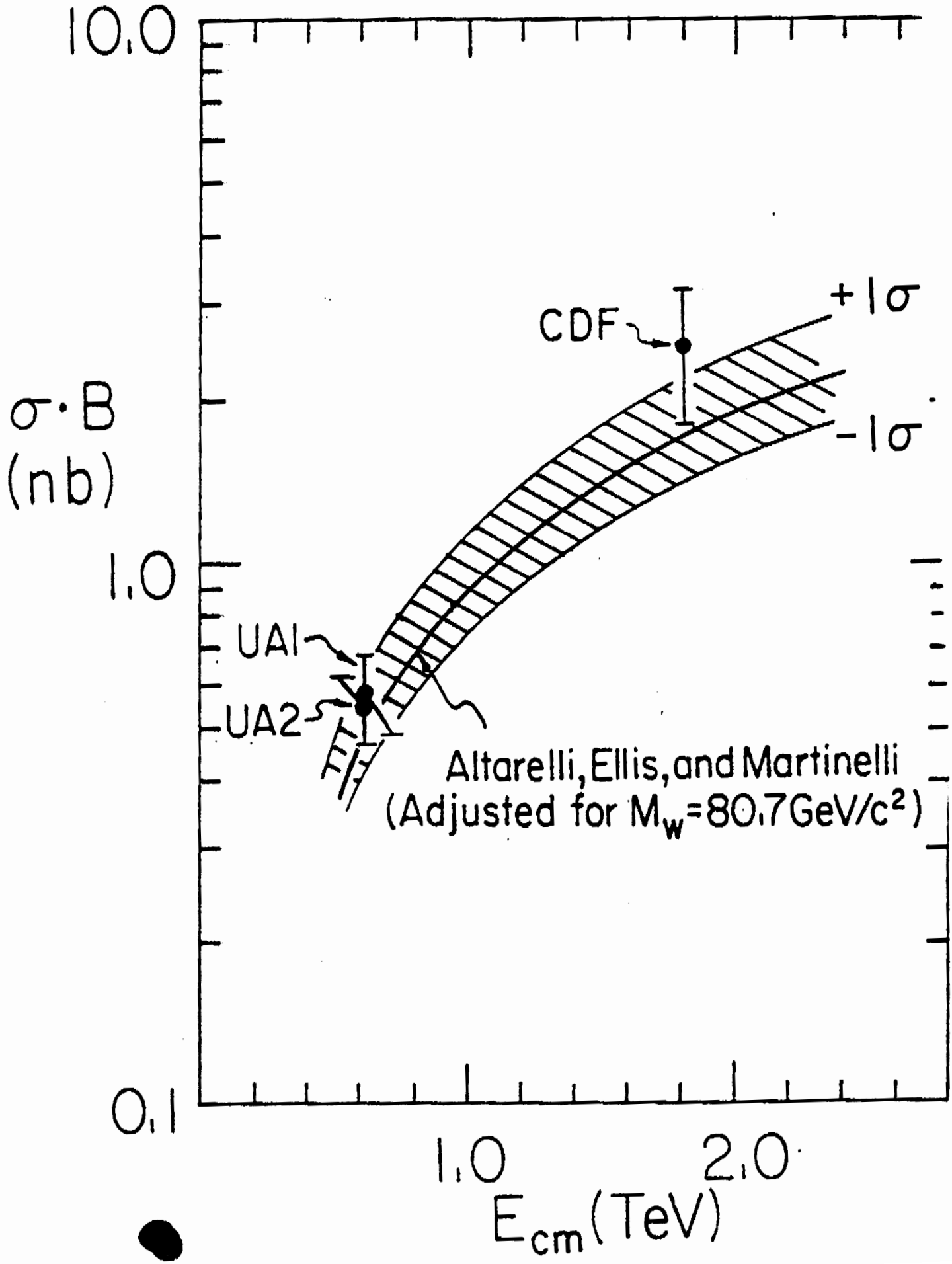
10.0
1.0
0.1
σ·B
(nb)
CDF
+1σ
-1σ
UA1
UA2
Altarelli, Ellis, and Martinelli
(Adjusted for M_W=80.7GeV/c^2)
1.0
2.0
E_{cm}(TeV)

FIGURE 4

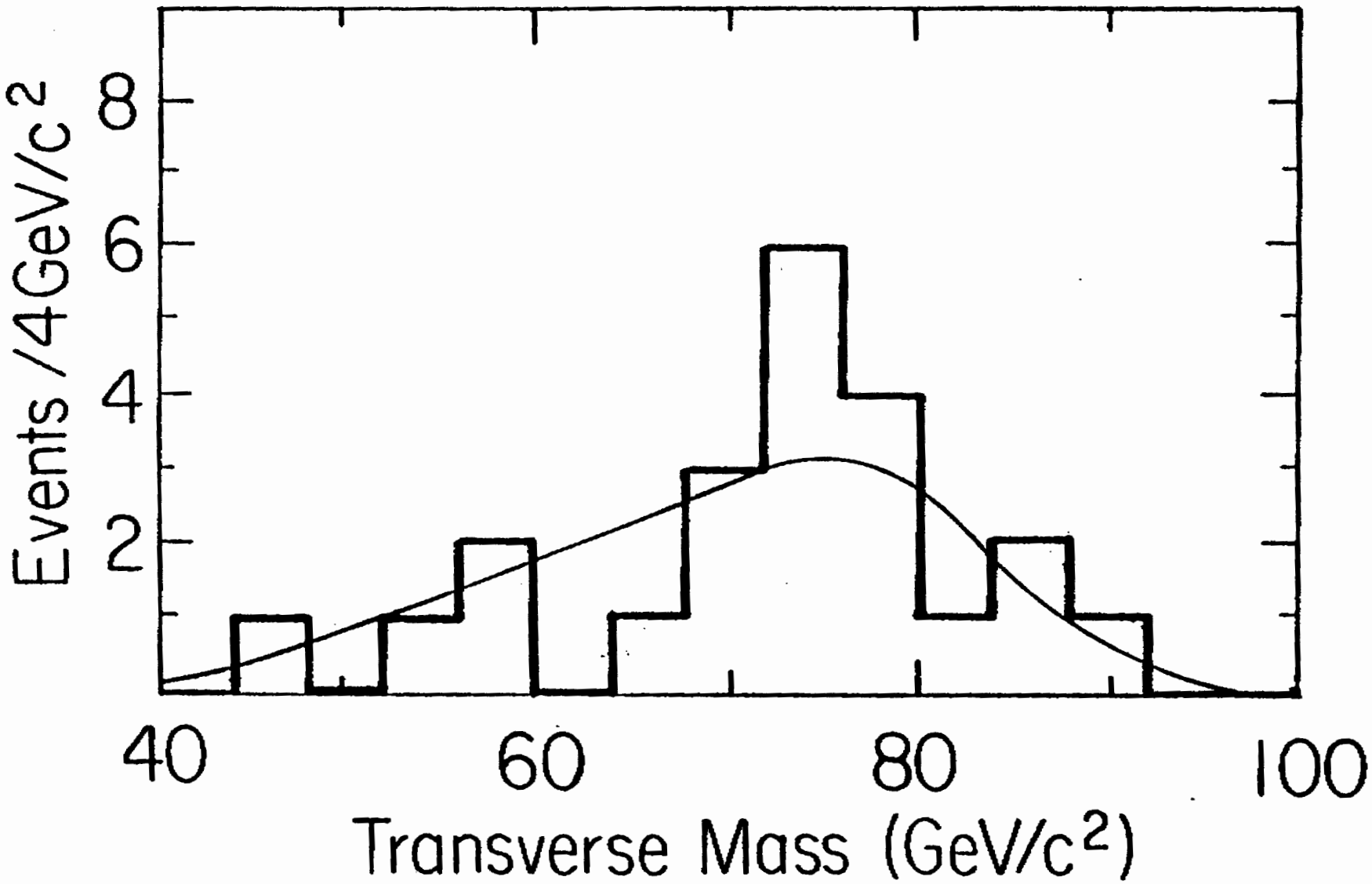

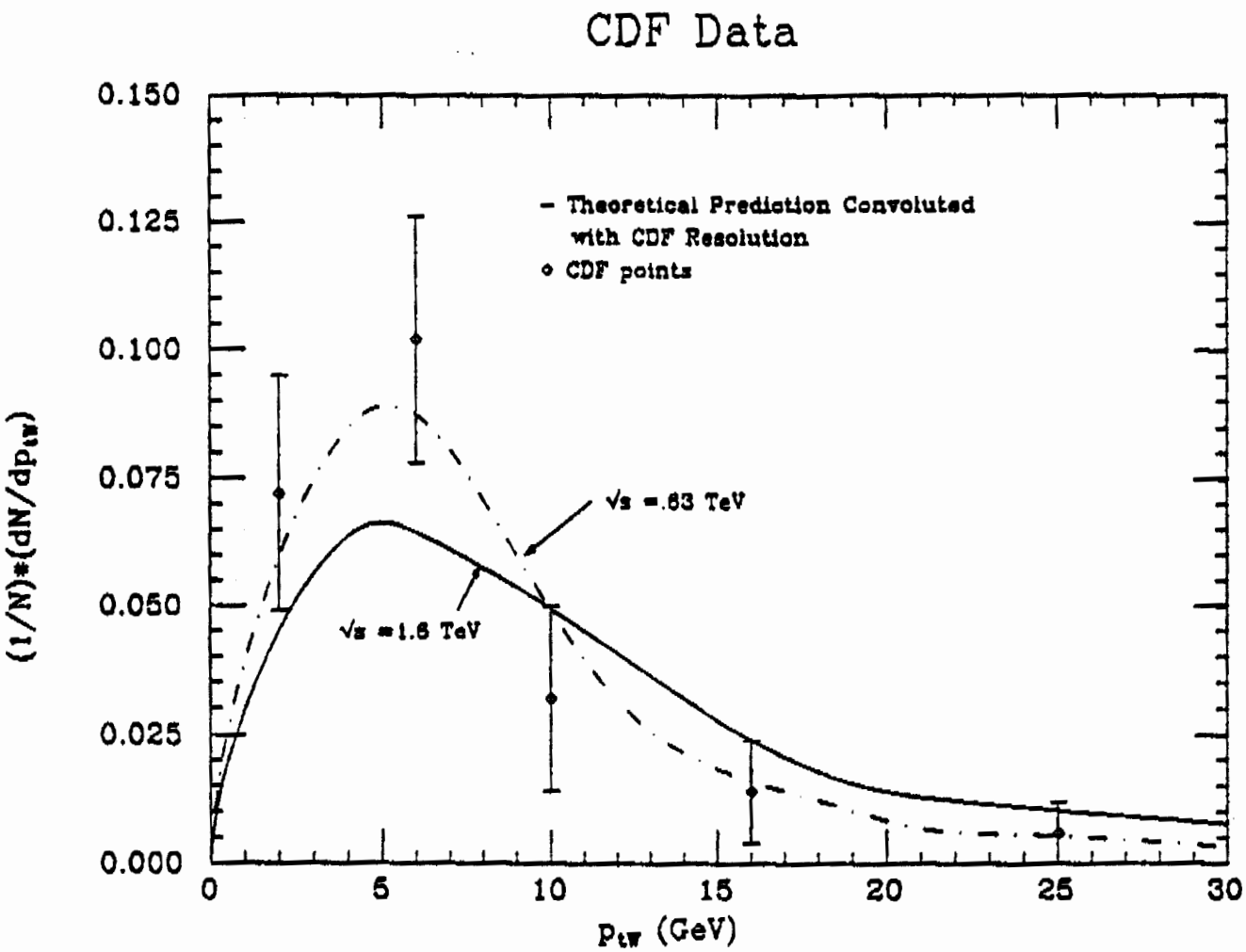
CDF Data
0.150
0.125
0.100
0.075
0.050
0.025
0.000
0
5
10
15
20
25
30
(1/N)*(dN/dp_tW)
p_tW (GeV)
– Theoretical Prediction Convoluted with CDF Resolution
◦ CDF points
√s =.63 TeV
√s =1.8 TeV

FIGURE 5